Journal of Genetic Engineering and Biotechnology 23 (2025) 100487

Contents lists available at ScienceDirect

Journal of Genetic Engineering and Biotechnology

journal homepage: www.elsevier.com/locate/jgeb

Virtual screening and identification of potent phytoconstituents from *Acorus calamus* L. as inhibitors of Monkeypox virus infection

Shivani Lakhani [a,1], Janki V. Rojmala [b,1], Nisarginee M. Chotai [b], Bhargav N. Waghela [b,*], Parth Thakor [a,*]

[a] Bapubhai Desaibhai Patel Institute of Paramedical Sciences, Charotar University of Science and Technology, Changa, Gujarat, India
[b] Faculty of Science, Atmiya University, Kalawad Road, Rajkot, Gujarat, India

ARTICLE INFO

Keywords:
Acorus calamus L.
A42R
A48R
D8L
D13L
Monkeypox

ABSTRACT

Background: The threat posed by the Monkeypox (Mpox) disease has re-emerged globally while the world strives to recover from the Corona Virus Disease −19 (COVID-19) pandemic. The World Health Organization has declared Mpox a global health emergency. Monkeypox virus (MPXV), the causative agent of Mpox disease, is a zoonotic, large, enveloped, double-stranded deoxyribonucleic acid (DNA) virus that belongs to the *Orthopoxviridae* genus. The Food and Drug Administration (FDA), USA has approved repurposed antiviral agents Cidofovir and Tecovirimat as the primary treatment options for Mpox, however, they project systemic toxicity and have underwhelming clinical data. A plethora of medicinal plant compounds including flavonoids, phenolics, terpenoids, and alkaloids have a wide range of biological activities such as antimicrobial, antioxidant, antiulcer, antineoplastic, anti-inflammatory, and immuno-stimulating potentials. Since many of them are being studied in modern research to discover an active drug candidate, we turned to medicinal plants to explore potent antiviral compounds.

Methods: In the present study, we aimed to screen phytoconstituents of *Acorus calamus* L. (AC) against four essential virulence enabling proteins D8L, A48R, D13L, and A42R of MPXV by *in silico* approach. Further, we have elucidated pharmaceutical-relevant parameters of hit compounds through their absorption, distribution, metabolism, excretion, and toxicity (ADMET) properties as well as drug-likeness parameters.

Results: Our results revealed that AC phytoconstituents such as β-Sitosterol against A42R and D8L, Lucenin-2 against D13L and Zingiberene against A48R showed the strongest binding affinities, respectively. Moreover, Galangin could prominently interact with all four proteins with lower binding energy and higher affinity. All top phytoconstituents obeyed Lipinski's RO5 and drug-likeness properties.

Conclusions: The phytoconstituents of AC can act as potent inhibitors of essential virulence enabling proteins of MPXV. Thus, we recommend further experimental investigations to validate the promising results of the present *in silico* study.

1. Introduction

Monkeypox virus (MPXV) is a zoonotic double-stranded DNA (~197 kb) virus that belongs to the *Orthopoxviridae* genus of the Poxviridae family and causes Monkeypox (Mpox) disease.[1] In 1958, the MPXV was first isolated from monkeys. Zoonosis of the MPXV was first observed in a 9-month-old boy from the Democratic Republic of the Congo in 1970, 12 years after its discovery.[1–2] Recently, Mpox has re-emerged in 2022 outside of its endemic areas, after repeated endemic outbreaks from 1971 to 2003.[1] According to previous reports, sporadic Mpox outbreaks occurred from 2003 to 2021 in various countries such as the USA, Israel, the UK, and Singapore.[1] WHO declared it as a public health emergency of international concern (PHEIC) twice, the first time in May 2022 and the second time in August 2024, as 120 countries reported over 100,000 confirmed cases and 220 deaths.[3–4] Recently in March 2024, India reported an endemic flare-up in Mpox cases.[5]

MPXV is a brick-shaped and enveloped virus consisting of surface tubular proteins, a dumbbell-shaped core component, and linear double-

* Corresponding authors at: Bapubhai Desaibhai Patel Institute of Paramedical Sciences, CHARUSAT, Changa, Gujrat, India.
E-mail addresses: wbhargav@gmail.com (B.N. Waghela), parth7218@gmail.com (P. Thakor).
[1] Authors Contributed Equally.

https://doi.org/10.1016/j.jgeb.2025.100487
Received 24 October 2024; Received in revised form 24 March 2025; Accepted 25 March 2025

stranded DNA fibrils surrounded by a rod-shaped palisade layer. The genome of MPXV is ~197 kb in length with 190 non-overlapping ORFs.[6] Phylogenetically, the virus is classified into two clades, Clade I and Clade II. Clades I and II have fatality rates of 3.6 % and 10.6 %, respectively. There is approximately a 0.5 % difference in the genomes of both virus clades. Particularly, the Clade IIb strain has been responsible for the global outbreak since 2022.[7–8]

The symptoms of MPXV infection manifest as skin rashes, fever, headache, body aches, nausea, and fatigue.[9] However, a distinguishing symptom of Mpox disease is lymphadenopathy. The rashes on cutaneous lesions progressively extend in the form of macules and papules to vesicles and pustules followed by crusting and scarring.[10–11] As seen for most poxviruses, MPXV enters host cells through three major stages: attachment, membrane fusion, and core invasion.[9] Several proteins play critical roles in the MPXV infection process, contributing to their ability to invade host cells and facilitate replication. Prominently, D8L, A48R, D13L, and A42R proteins facilitate cell entry, viral replication, assembly, and the catalysis of the envelopment of intracellular mature virus particles in MPXV respectively.[6] D8L plays a crucial role in viral entry by allowing the attachment and fusion of MPXV.[12] A48R, a thymidylate kinase is involved in the synthesis of nucleotides and D13L, which helps in virus morphogenesis.[13–15] A42R is a profilin-like protein that helps in the motility and development of viral cells.[16] MPXV evades the host immune system by numerous viral proteins interfering with key antiviral pathways and mechanisms. Through these proteins, MPXV can escape from apoptosis and cannot be detected by antiviral chemokines. They also modulate the expression and function of innate immune mediators such as interferons, interleukins, toll-like receptors, and reduce cellular activation. MPXV also disrupts the key transcription factors that regulate the expression of inflammatory genes such as IFNα/β and IRF3. MPXV blocks the activation of the Complement and Pattern Recognition Receptors (PRR) cascade as well and prevents NF-κB activation. The virulent proteins of MPXV can inactivate inflammatory molecules such as TNFα, IFNγ, IL-1β, IL-18, and IL-6. MPXV increases its replication and infection into the host cells by suppressing or altering the immune response, resulting in tissue damage, systemic inflammation, and organ failure.[17–22]

According to the Centre for Disease Control and Prevention (CDC), USA, no dedicated treatment is available for MPXV infections. However, the vaccinia vaccines and several antivirals used to treat smallpox are being considered as potential therapeutic agents for MPXV. Few live attenuated vaccines such as MVA-BN (Modified Vaccinia Ankara-Bavarian Nordic), LC16m8, and ACAM2000 are approved as preventive measures for MPXV infection as per NIAID-NIH Report. However, MVA-BN causes severe side effects in people having weakened immune systems and individuals with eczema. ACAM2000 is not recommended for any group of atopic dermatitis, immunocompromised individuals, and pregnant women.[23–24] Antivirals such as Tecovirimat (an inhibitor of intracellular viral release), Cidofovir (a DNA polymerase inhibitor), and Brincidofovir (a prodrug for Cidofovir) are generally utilized for the treatment of Mpox disease. However, the efficacies of Tecovirimat, Cidofovir, and Brincidofovir against the MPXV are ambiguous. Tecovirimat is an FDA-approved drug for smallpox treatment but it has underexplored safety or efficacy data available for Mpox treatment.[25] Cidofovir was originally used to treat cytomegalovirus (CMV) retinitis in AIDS patients, and demonstrated several adverse effects including renal, gastrointestinal, and hepatotoxicity when used for Mpox treatment.[26] Hence, it became necessary to study effective and safer compounds for the therapeutic regimen of Mpox. Since Indian medicinal plants present time-tested and valid therapeutic potential, screening of plant-originated molecules may lead to exceptionally potent, target-specific, and effective drug compounds.

Acorus calamus L. (AC) is a perennial herbaceous plant, commonly referred to as sweet flag or calamus or 'Vacha' holds therapeutic importance since ancient ethnomedicinal practices.[27] Traditionally, AC has been used to treat neurological, metabolic, gastrointestinal, and other health disorders.[28] In line, major phytoconstituents of AC such as α-Asarone, β-Asarone, Galangin, and others demonstrate a variety of bioactivities including antimicrobial, antioxidant, anti-inflammatory, blood glucose-lowering, and anti-tumor effects.[27,29] Earlier reports predict the effectiveness of AC phytoconstituents against Severe Acute Respiratory Syndrome Coronavirus-2 (SARS-CoV-2), Dengue virus, Ebola, and Nipah virus through *in silico* approaches.[30–33] In the present study, we have employed an *in silico* molecular docking approach to analyze the potency of 255 phytoconstituents present in AC against MPXV target proteins i.e., D8L, A48R, D13L, and A42R. Further, we have investigated the ADMET parameters to measure the efficacy and safety of the AC phytoconstituents.

2. Materials and Methods

2.1. Retrieval of Monkeypox virus proteins

To assess the antiviral potential of phytoconstituents from AC against the MPXV, we focused on the important virulent proteins such as cell surface binding-envelope protein D8L, Thymidylate kinase A48R, viral capsid protein D13L, and a profilin-like protein A42R. The 3D structures of D8L (PDB ID: 4E9O), A48R (PDB ID: 2V54), D13L (PDB ID: 6BED), A42R (PDB ID: 4QWO) were retrieved from the RCSB protein data bank in .pdb file format.[34] Using Discovery Studio 2024,[35] the downloaded .pdb structures of the proteins were refined by removing heteroatoms and water molecules as well as the addition of polar hydrogen atoms. Subsequently, protein structures were saved in .pdb format which were used for molecular docking in PyRx 0.8.[36]

2.2. Retrieval of phytoconstituents and library preparation

The phytoconstituents of AC have been known for their wide range of pharmacological properties and therapeutic applications. Hence, our study aimed to explore the antiviral efficiency of AC phytoconstituents. A list of the phytoconstituents was downloaded from the IMPPAT 2.0 (Indian Medicinal Plants, Phytochemistry, and Therapeutics 2.0) database.[37] IMPPAT 2.0 is an enhanced and expanded database having manually curated information on 4010 Indian medicinal plants, 17,967 phytochemicals, and 1095 therapeutic uses. This specialized database enables in-depth exploration and analysis of the botanical landscape of India for drug discovery and therapeutic purposes. A library of all the phytoconstituents has been prepared from the database. The 3D structures of phytoconstituents were downloaded in .sdf format from the PubChem database which is a comprehensive database maintained by the National Center for Biotechnology Information (NCBI). PubChem database is generally used to access the structures of a broad range of chemical compounds. It also provides information about their molecular formula, molecular weight, and other details. Obtained 3D structures of phytoconstituents were inserted using open babel (inbuilt under PyRx 0.8) and preparation of the final ligand by minimizing them and converting it to autodock ligand (.pdbqt) was done.

2.3. Virtual screening of compounds by molecular docking against Monkeypox virus proteins

Virtual screening is a computational technique generally used in drug discovery that is employed to identify potential hit candidates by using a large database or collection of compounds against a specific receptor to identify the effective therapeutic candidate.[38] Molecular docking is used in the CADD (computer-aided drug design) process, which predicts the affinity and binding pose of a ligand and targeted macromolecule.[39] We used PyRx 0.8, which is virtual screening software that aids in the rapid screening of large compound libraries at the same time against one macromolecule, which enables saving time and effort as PyRx requires no command line because it is automated. A library of 255 compounds of AC was screened using Autodock Vina Wizard against

four different macromolecules by docking. We also used standard drugs as controls : Diosmin and Mitoxantrone, specific to D8L and A42R respectively.[40–41] Also, Dolutegravir, Cinacalcet, and Doxorubicin specific to A48R[42] were docked to generate binding affinity scores. Tecovirimat has been proven to be effective against MPXV[26] and was used as a standard common drug to be screened against all four receptors. The grid box for D8L and A48R was defined with the parameters of X = 21.6002, Y = 5.4329, Z = 1.4904, and X = 4.6263, Y = 16.0524, Z = 1.7350, respectively, and their dimensions were set to 25 Å for XYZ. The grid box for D13L was defined by X = 89.1030, Y = 96.7728, Z = 5.5933 and dimensions were maximized up to X = 66.0671 Å, Y = 56.2946 Å, and Z = 99.0486 Å. The A42R grid box parameters were set to X = 3.3904, Y = 4.2831, Z = 14.3660 and dimensions were maximized up to X = 52.897 Å, Y = 59.5304 Å, and Z = 37.9783 Å. Virtual screening was run using default setup parameters and a default exhaustiveness value 32, and the top 15 drug candidates with the highest negative binding energy (kcal/mol) were selected against each macromolecule. Selected top fifteen ligands were re-docked, and the pose with the highest negative binding energy and RMSD value 0 Å were considered. Selected docked ligands were displayed and the top best model (model 1) out of nine, which had higher negative binding energy was saved in a .pdb file. Docked ligand and protein structure molecular interactions were visualized using Discovery Studio 2024 and a 2D diagram of receptor-ligand was generated.

2.4. Prediction of drug-like properties

Understanding the drug-like properties of novel drug candidates is essential for their evaluation. These characteristics are required to predict how well a drug will function inside the body. The SwissADME webserver was used in this study to assess the physicochemical characteristics, lipophilicity, and drug-likeness properties of the chosen compounds after the virtual screening process.[43] Identifying compounds suitable for drug use involves adhering to specific rules such as Lipinski's,[44] Veber's,[45] and Egan's.[46] Compounds that disrupt the Lipinski, Veber, and Egan rules multiple times may have problems with their ADMET parameters. Lipinski, Veber, and Egan's criteria are met by only <10 % of drugs that make it to clinical trials. In addition, we have evaluated two more factors: topological polar surface area (TPSA) and number of rotatable bonds (nROTB).[47] These criteria can be used to determine whether the drug molecule has flexible or inflexible interactions with the specific receptor.

2.5. Prediction of ADMET properties

Drug development is challenging when prospective therapeutic agents have poor pharmacokinetic and safety characteristics, which increases the failure rate of moving on to clinical trials. Computational techniques can ably address these issues and alleviate them significantly. The research and reports underscore the noteworthy advantages of employing ADMET for forecasting drug molecule pharmacokinetics and toxicity parameters prior to clinical or preclinical trials.[48–49] A useful and free tool for forecasting the pharmacokinetic qualities of medications, such as their absorption, distribution, metabolism, and excretion (ADME) features, is the web-based server pkCSM.[50] Using this machine learning technique, we examined our screened compounds' ADME parameters. We assessed the compounds' various ADME characteristics, such as water solubility (Log S), human intestinal absorption, the permeability of the blood–brain barrier (BBB), CYP450 substrates, and CYP450 inhibitors.

Examining the toxicological characteristics of the selected natural compounds was crucial, given the possible hazards associated with medicine. The pkCSM online server, widely known for their efficacy in drug discovery, were also used to predict the toxicological analysis of particular compounds. The compounds were filtered using parameters like oral rat acute toxicity, human ether-a-go-go-related gene, and AMES toxicity.

3. Results

3.1. Phytoconstituents of A. calamus L. Exhibit high binding affinity to protein targets of MPXV

In the present study, we evaluated the binding affinity of the 255 phytoconstituents from AC against the protein targets of MPXV by a molecular docking approach. We used the PyRx virtual screening tool to predict the interactions between reported phytoconstituents and various proteins of the MPXV such as D8L, A48R, D13L, and A42R. These proteins are reported to play a vital role in viral entry (D8L), viral replication (A48R), morphogenesis of immature virions (D13L), and viral spreading (A42R).[16,51–53] PyRx provides ligand-receptor molecular docking results as 9 different poses with respective binding energy. The pose with the least binding energy indicates the strongest interaction.[54] The compounds with lower binding energies and hence the strongest interactions were considered for further analysis.

3.1.1. In silico screening of A. calamus L. Phytoconstituents targeting D8L

D8L plays a crucial role in viral entry by allowing the attachment and fusion of MPXV with the host cell, thereby initiating its infection.[51] In the present study, 13 phytoconstituents of AC have demonstrated an acceptable binding affinity (≤ −6.2 kcal/mol), which is analogous to Diosmin (−8.5 kcal/mol) and Tecovirimat (−8.1 kcal/mol). Moreover, a large number of favourable hydrogen and hydrophobic bonds are involved in the interaction of AC phytoconstituents with D8L. Among the screened compounds, β-Sitosterol displayed the highest docking score (−7.6 kcal/mol). Followed by Lucenin-2 (−7.1 kcal/mol), Galangin (−6.9 kcal/mol), Mukulol (−6.9 kcal/mol), (+)-delta-Cadinene (−6.5 kcal/mol), [(1S,3R,5S,8S,9R,11R,14R,16S,17R,18S,19S)-9,10,19-trihydroxy-5-methyl-12-methylidene-7-azaheptacyclo[9.6.2.01,8.05,17.07,16.09,14.014,18]nonadecan-3-yl] acetate (−6.5 kcal/mol), Benzyl benzoate (−6.5 kcal/mol), and Chalcone (−6.5 kcal/mol) respectively with D8L. In addition, (−)-alpha-Cadinol, (1S,4S)-1,4-dimethyl-7-propan-2-ylidene-1,2,3,4,5,8-hexahydroazulen-6-one, β-Cubebene, *cis*-Calamenen-10-ol, and Heterotropan presented a moderate docking score, −6.3 kcal/mol (Table 1). All 13 compounds interacted with D8L through multiple hydrogen and hydrophobic interactions (Table 1). Briefly, THR 173, ARG 44, TYR 69, ILE 174, ASN 175, HIS 67, and LEU 42 were predicted to be the key amino acids involved in interactions with almost all phytoconstituents (Fig. 1 and Table 1). These amino acids also play an important role in the interactions between Diosmin-D8L or Tecovirimat-D8L complexes (Supplementary Table S5). Moreover, β-Sitosterol interacted with D8L through favorable interactions by THR 39, THR 173, LYS 41, LYS 108, ARG 44, ARG 220, SER 64, SER 65, TYR 69, VAL 94, GLU 105, ILE 174, ASN 175, LEU 42, HIS 67, and TYR 104. Other studied phytoconstituents with moderate docking scores have been summarized in Supplementary Table S1 and Supplementary Fig. S1. Based on the docking scores and interactions analysis, it can be predicted that β-Sitosterol, Lucenin-2, and Galangin may act as potent inhibitors of the D8L.

3.1.2. In silico screening of A. calamus L. Phytoconstituents targeting A48R

A48R phosphorylates thymidine monophosphate and converts it into diphosphate.[4] Thymidylate kinase phosphorylates 50 halogenated deoxyuridine monophosphate (dUMP) analogs. A48R plays an important role in viral replication by being involved in nucleotide metabolism and could be the prominent target to eradicate MPXV infection.[55] In this study, we docked phytoconstituents of AC against A48R. Cinacalcet and Tecovirimat were taken as control. Our findings revealed that compounds Zingiberene (−8.6 kcal/mol), β-Bisabolene (−8.5 kcal/mol), Galangin (−8.5 kcal/mol), and (+)-delta-Selinene (−8.4 kcal/mol) displayed excellent binding energies with values below −8.3 kcal/mol which were similar to Cinacalcet (−9.5 kcal/mol) and Tecovirimat

Table 1
Phytoconstituents of *A. calamus* L. with higher docking scores and their amino acids interaction profile with target protein D8L (PDB ID: 4E9O).

Receptor Name	Name of Compound	Docking Score (kcal/mol)	Types of interactions with amino acid residues				
			Van der Waals	Alkyl	Pi interactions	Conventional H-bond	Carbon-hydrogen bond
4E9O	beta-Sitosterol	−7.6	THR 39, 173 LYS 41, 108, ARG 44, 220 SER 64, 65, TYR 69, VAL 94, GLU 105, ILE 174, ASN 175	LEU 42	Pi-Sigma: TYR 104 Pi-alkyl:HIS 67,TYR 104		
	Lucenin-2	−7.1	THR 39, 173, ARG 44, 220, SER 64, 177 ASN 92, 218 VAL 94, TRP 182, ILE 116, 174, LEU 114,LYS 108		Pi-Sigma: LEU 42, Pi-alkyl: LEU 42 Pi-Pi Stacked: TYR 104 Pi-Pi T-shaped: HIS 67	SER 65, TYR 69,TYR 104,ASN 175	
	Galangin	−6.9	LEU 42, TYR 69, 104 SER 65, 177, HIS 67, THR 173, ILE 174, ASN 175,		Pi-Cation: ARG 44	ASN 46, SER 64, GLU 105,LYS 108	
	Mukulol	−6.9	THR 39, 173, LEU 42, ARG 44, 220 SER 65, 177, TYR 69, TYR 104, LYS 108, ASN 175	VAL 94, ILE 116, ILE 174	Pi-alkyl: HIS 67		
	(+)-delta-Cadinene	−6.5	THR 39, 173,ASN 175, 218, ARG 220	LEU 42, HIS 67, TYR 69, ILE 174			
	[(1S,3R,5S,8S,9R,11R,14R,16S,17R,18S,19S)-9,10,19-trihydroxy-5-methyl-12-methylidene-7-azaheptacyclo [9.6.2.01,8.05,17.07,16.09,14.014,18]nonadecan-3-yl] acetate	−6.5	ARG 44, ASN 46, HIS 67, THR 173, SER 177		Pi-Sigma: TYR 104	SER 65,LYS 108, ASN 175	GLU 105
	Benzyl benzoate	−6.5	SER 64, 65, TYR 69, ASN 92,ILE 116, 174, THR 173		Pi-Cation: ARG 44, Pi-alkyl: VAL 94 Pi-Pi Stacked: TYR 104 Pi-Pi T-shaped: HIS 67		
	Chalcone	−6.5	LEU 42, TYR 69, 104, ILE 116, 174,ASN 175,ARG 220		Pi-Sigma: THR 173, Pi-alkyl: LYS 41,VAL 94 Pi-Pi T-shaped: HIS 67		

(*continued on next page*)

Table 1 (*continued*)

Receptor Name	Name of Compound	Docking Score (kcal/mol)	Types of interactions with amino acid residues				
			Van der Waals	Alkyl	Pi interactions	Conventional H-bond	Carbon-hydrogen bond
	(−)-alpha-Cadinol	−6.3	ARG 44, 220,THR 173,ASN 175	LYS 41, LEU 42, ILE 174	Pi-alkyl: HIS 67,TYR 69	THR 39	
	(1S,4S)-1,4-dimethyl-7-propan-2-ylidene-1,2,3,4,5,8-hexahydroazulen-6-one	−6.3	THR 39, 173 ARG 44, 220 HIS 67, TYR 69,ILE 174,ASN 175	LYS 41, LEU 42			
	beta-Cubebene	−6.3	THR 39, TYR 69, ILE 174, ASN 175, 218,ARG 220	LEU 42			
	cis-Calamenen-10-ol	−6.3	THR 39, 173, ARG 44, 220, TYR 69	ILE 174	Pi-Sigma: LEU 42, ASN 175 Pi-alkyl:LYS 41,HIS 67		
	Heterotropan	−6.3	THR 39, 173, LYS 108, LEU 114, ILE 174, ASN 175, ARG 220	LEU 42, ARG 44, VAL 94, ILE 116	Pi-alkyl: HIS 67,TYR 104,LYS 41	TYR 69	LYS 41

(−10 kcal/mol) (Table 2 and Supplementary Table S5). Other than that, phytoconstituents such as Benzyl benzoate, Indane, 1-phenyl, alpha-Selinene, (−)-β-Curcumene, and Chalcone also showed upstanding affinity by showing binding energies lower than −8.1 kcal/mol (Table 2). The maximum number of hydrogen bonds and hydrophobic interactions can be seen between phytoconstituents and amino acid residues ARG 72, ARG 93, SER 97, GLY 98, PRO 39, LEU 53, TYR 101, and TYR 144 (Fig. 2 and Table 2). Zingiberene showing the highest docking score, was stabilized by van der Waals interaction with ASP 13, PHE 38, PRO 39, VAL 64, ASN 65, ARG 72, ARG 93, SER 97, GLY 98, GLU 142, and hydrophobic interaction with LEU 53, TYR 101, TYR 144, ALA 102, LYS 105, and PHE 68. The phytoconstituents having a higher binding affinity towards A48R have been summarized (Table 2 and Fig. 2). Further, phytoconstituents with moderate docking scores are depicted (Supplementary Fig. S2 and Supplementary Table S2). Overall, our results suggest that Zingiberene, β-Bisabolene, Galangin, and (+)-delta-Selinene remarkably interact with A48R.

3.1.3. *In silico screening of A. calamus L. Phytoconstituents targeting D13L*

D13L is a scaffold protein of pox viruses and is crucial in viral morphogenesis.[53] Moreover, D13L is a highly conserved sequence throughout pox virus genomes and has played an essential role in the formation of mature cell-associated enveloped virus (CEV) or the free extracellular enveloped virus (EEV). The docking result of the AC phytoconstituents against D13L revealed that the binding energies of Lucenin-2 and Galangin were −9.2 kcal/mol and −8.7 kcal/mol respectively, almost at par with the binding energy of Tecovirimat (−10.6 kcal/mol). Galangin and other compounds having binding energy less than −7.4 kcal/mol displayed favorable bond interactions as hydrogen bonds and hydrophobic bonds with the amino acid residues PRO 88, TYR 89, TYR 283, ASN 435, ASN 472, GLN 278, ILE 120, PHE 433 and LYS 429. All these amino acid residues also showed interactions with Tecovirimat (Fig. 3 and Table 3). Our study revealed that interactions between Lucenin-2 and the D13L protein were predominantly stabilized by several favorable interactions with amino acids ASN 96, ASN 424, ILE 95, ILE 428, GLU 111, GLY 112, PRO 186, PRO 426, ARG 234, ILE 236, LYS 260, TYR 262, PHE 427, GLN 524 in form of van der Waals attractions. Additionally, ASP 189 and PRO 426 were involved in Pi interactions and ASN 185, ASN 268, PRO 261, PRO 426, TYR 263, and ASP 425 formed conventional hydrogen bonds. Furthermore, most of the amino acids of the Lucenin-2-D13L complex were not involved in the Tecovirimat-D13L complex (Table 3 and Supplementary Table S5). All the other interactions with moderate binding affinity between phytoconstituents and D13L are briefly summarized in Supplementary Table S3 and visualization of these interactions is depicted in Supplementary Fig. S3. Consequently, it can be prophesied that phytoconstituents such as Lucenin-2, Galangin, and Spathulenol can potentially inhibit D13L.

3.1.4. *In silico screening of A. calamus L. Phytoconstituents targeting A42R*

The A42R, a profilin-like protein of the MPXV is involved in viral motility and its spread to adjoining cells. A42R is greatly conserved in Orthopoxviruses and this makes it a crucial drug target.[16] Amongst all, β-Sitosterol, (2S,3R,4R,5S,6S)-2-(hydroxymethyl)-6-(((2S,3R,4R,5S,6R)-3,4,5-trihydroxy-6-(((4aR,8aS)-4-isopropyl-1,7-dimethyl-1,2,3,4,4a,5,8,8a-octahydronaphthalen-1-yl)oxy)tetrahydro-2H-pyran-2-yl)methoxy)tetrahydro-2H-pyran-3,4,5-triol, Lucenin-2 and [(1S,3R,5S,8S,9R,11R,14R,16S,17R,18S,19S)-9,10,19-trihydroxy-5-methyl-12-methylidene-7-azaheptacyclo[9.6.2.01,8.05,17.07,16.09,14.014,18]nonadecan-3-yl]acetate could fit well into the active site pocket of A42R with binding energy −8.8 kcal/mol, −8.7 kcal/mol, −8.5 kcal/mol, and −8.0 kcal/mol which is higher than the control Mitoxantrone (−7.4 kcal/mol) and nearly same as tecovirimat (−8.9 kcal/mol) (Table 4). A network of hydrogen bonds and hydrophobic interactions stabilized A42R-ligand complexes. Amino acid residues such as THR A: 79, ARG B:

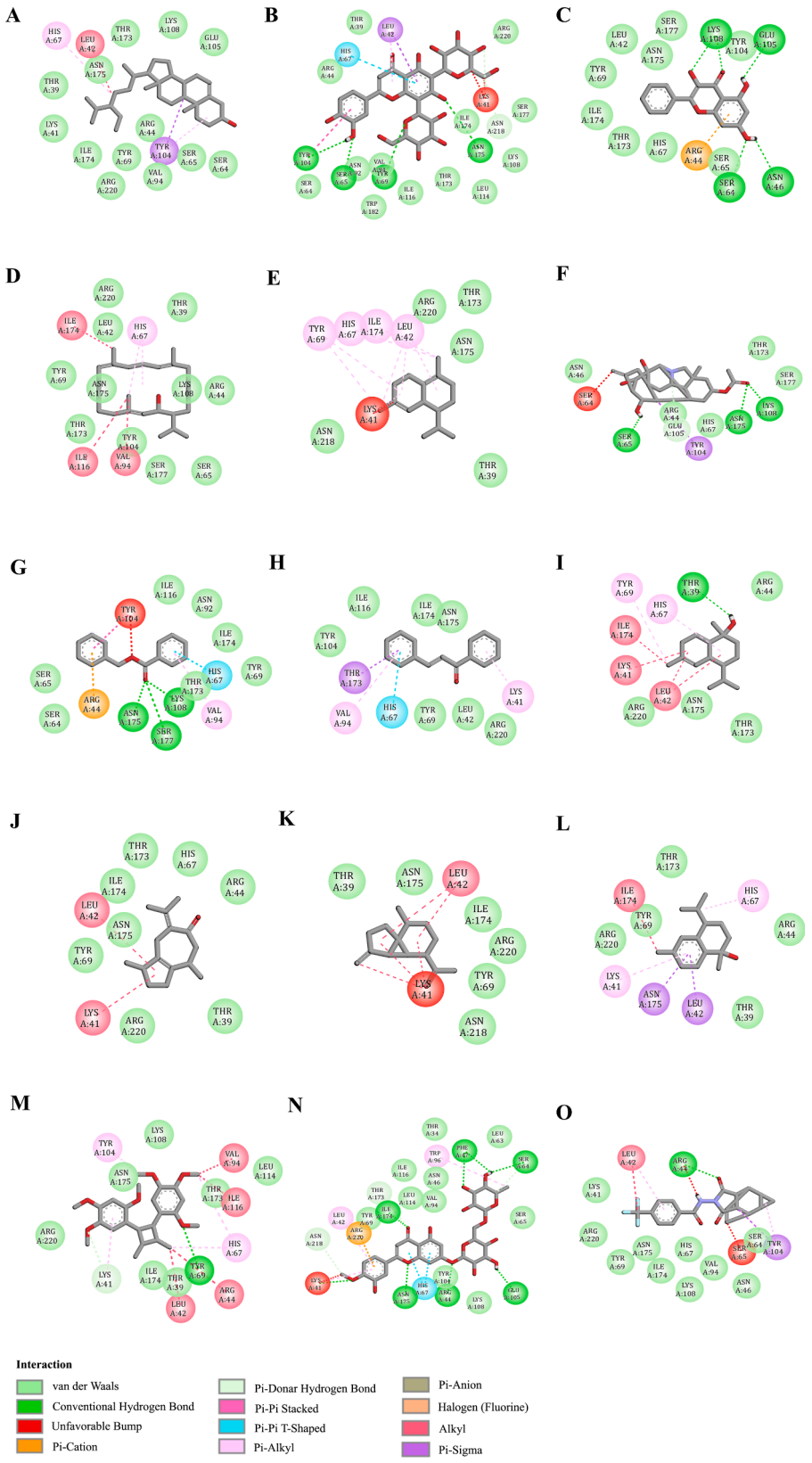

Fig. 1. Molecular 2D interaction of D8L (PDB ID: 4E9O) with phytoconstituents of *A. calamus* L. having binding energy ≤−6.3 kcal/mol (A) β-Sitosterol (B) Lucenin-2 (C) Galangin (D) Mukulol (E) (+)-delta-Cadinene (F) [(1S,3R,5S,8S,9R,11R,14R,16S,17R,18S,19S)-9,10,19-trihydroxy-5-methyl-12-methylidene-7-azaheptacyclo [9.6.2.01,8.05,17.07,16.09,14.014,18]nonadecan-3-yl] acetate (G) Benzyl benzoate (H) Chalcone (I) (−)-alpha-Cadinol (J) (1S,4S)-1,4-dimethyl-7-propan-2-ylidene-1,2,3,4,5,8-hexahydroazulen-6-one (K) beta-Cubebene (L) *cis*-Calamenen-10-ol (M) Heterotropan. Standard antibiotics (N) Diosmin with binding energy −8.5 kcal/mol and (O) Tecovirimat with binding energy −8.1 kcal/mol were utilized as control.

Table 2
Phytoconstituents of *A. calamus* L. with higher docking scores and their amino acids interaction profile with thymidylate kinase A48R (PDB ID: 2V54).

Receptor Name	Name of Compound	Docking Score (kcal/mol)	Types of interactions with amino acid residues				
			Van der Waals	Alkyl	Pi interactions	Conventional H-bond	Carbon-hydrogen bond
2V54	Zingiberene	−8.6	ASP 13, PHE 38, PRO 39, VAL 64, ASN 65, ARG 72, 93, SER 97,GLY 98,GLU 142	LEU 53, ALA 102,LYS 105	Pi-Sigma: PHE 68 Pi-alkyl:TYR 101, 144,PHE: 68		
	beta-Bisabolene	−8.5	ASP 13, PHE 38, PRO 39, VAL 64, ASN 65, ARG 72, ARG 93,SER 97, GLY 98, GLU 142		Pi-alkyl: LEU 53, PHE 68, TYR 101, 144, ALA 102, LYS 105		
	Galangin	−8.5	ASN 37, PHE 38, LEU 53, ARG 72, SER 97, GLY 98,TYR 144, GLU 145		Pi-Cation: ARG 41, 93 Pi-alkyl: PRO 39 Pi-Pi stacked: PHE 68 T shaped: TYR 101	GLU 142	
	(+)-delta-Selinene	−8.4	LYS 17, ASN 37, PHE 38, ARG 41, 72, 93, SER 97, GLY 98,GLU 142, TYR 144	PRO 39,LEU 53	Pi-Sigma: TYR 101 Pi-alkyl:PHE 68, TYR 101		
	Benzyl benzoate	−8.2	ASP 13, PRO 39, VAL 64, ASN 65,GLY 98,LYS 105		Pi-Pi stacked and amide-pi stacked: PHE 68, TYR 101 Pi-Pi T-shaped: TYR 144, TYR 101 Pi-alkyl: LEU 53,ALA 102	ARG 72	SER 97
	Indane, 1-phenyl	−8.2	ASP 13, ARG 41, 72, 93, SER 97, GLY 98,TYR 144	LEU 53,	Pi-Pi stacked: PHE 68 Pi-anion: GLU 142 Pi-alkyl: PRO 39,TYR 101,LEU 53		
	alpha-Selinene	−8.2	ASN 37, PHE 38, ARG 41, 72, 93, SER 97, GLY 98, GLU 142,TYR 144	PRO 39,LEU 53,	Pi-Sigma: TYR 101 Pi-alkyl:PHE 68,TYR 101		
	(−)-beta-Curcumene	−8	ASP 13, SER 97, GLY 98, ASN 65, VAL 64, PRO 39,ARG 93, GLU 142	LEU 53,ALA 102,LYS 105	Pi-Pi T shaped: TYR 101,144 Pi-alkyl:PHE 68,TYR 144		
	Chalcone	−8	ASP 13, LYS 17, ASN 37, PHE 38, PRO 39, ARG 41, 72 LEU 53, SER 97, GLY 98,TYR 101, 144,GLU 142		Pi-Pi stacked: PHE 68 Pi-Cation: ARG 93		

115, TYR A: 118, TYR B: 118, ARG B:119, ARG A: 119, ARG A:122, and ARG B: 122 have a crucial role in interactions between most of the phytoconstituents and A42R (Table 4 and Fig. 4). Above mentioned amino acids are also key molecules for Mitoxantrone and Tecovirimat complexes with A42R (Supplementary Table S5). Phytoconstituents (1S,4S)-1,4-dimethyl-7-propan-2-ylidene-1,2,3,4,5,8-hexahydroazulen-6-one, Arhimachalene, gamma-Diasarone, and Thunbergol also showed significant docking score against A42R bound to the key amino acids of A42R active site.

2D interaction analysis for one of the most active compounds β-Sitosterol indicated a series of favourable van der Waals bonds with THR A:71, THR A: 79, SER A:73, GLU A:83, ARG A:114, ARG B:115, and ASP B:123. Pi alkyl/alkyl interactions with amino acids TYR A:118, ARG A:119, ARG A:122, TYR B:118, ARG B:119, and ARG B:122 were also

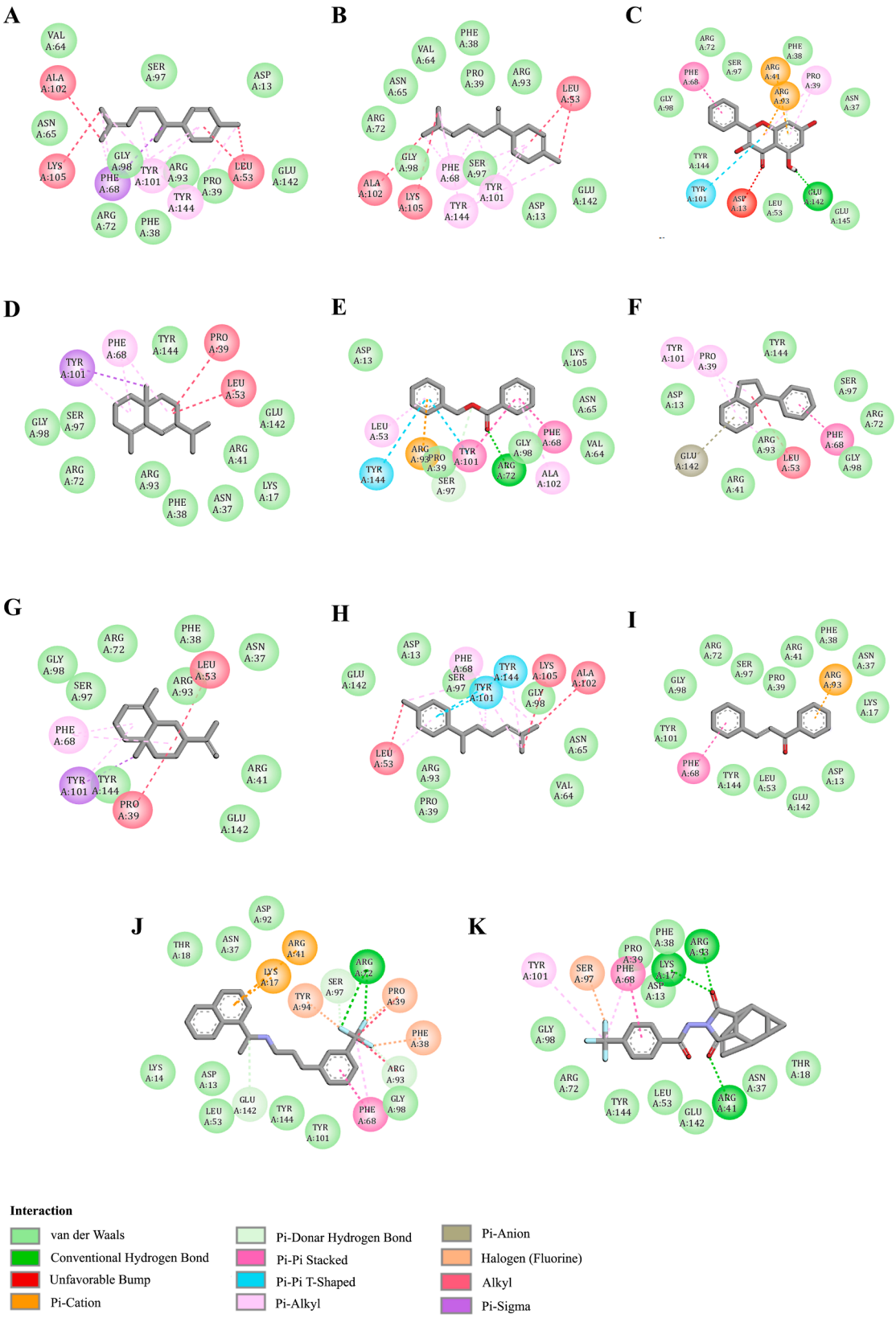

Fig. 2. Molecular 2D interaction of A48R (PDB ID: 2V54) with phytoconstituents of *A. calamus* L. having binding energy ≤−8.0 kcal/mol (A) Zingiberene (B) β-Bisabolene (C) Galangin (D) (+)-delta-Selinene (E) Benzyl benzoate (F) Indane, 1-phenyl (G) alpha-Selinene (H) (−)-beta-Curcumene (I) Chalcone. Standard antibiotics (J) Cinacalcet with binding energy −9.5 kcal/mol and (K) Tecovirimat with binding energy −10.0 kcal/mol were utilized as control.

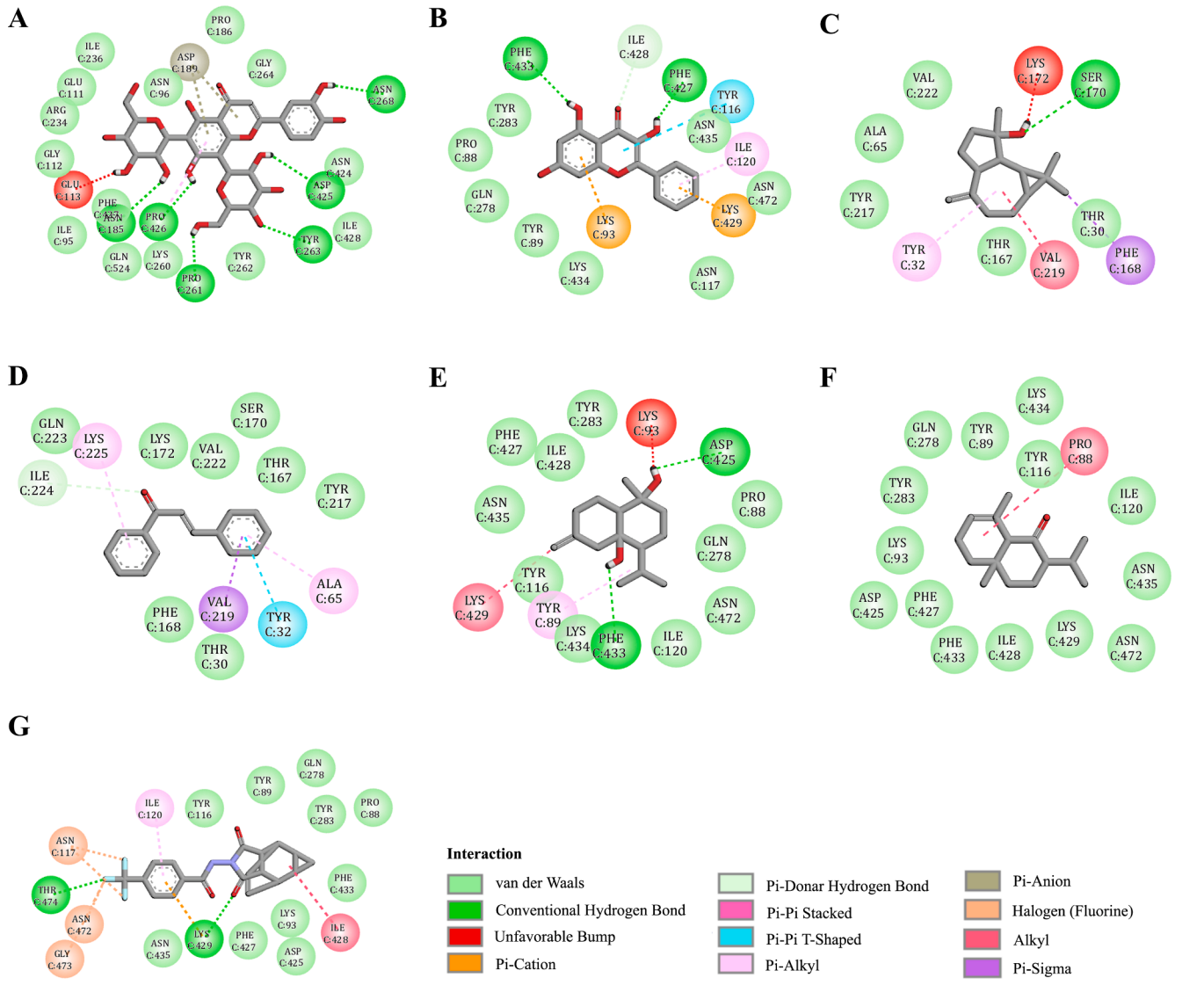

Fig. 3. Molecular 2D interaction of D13L (PDB ID: 6BED) with phytoconstituents of *A. calamus* L. having binding energy ≤−7.5 kcal/mol (A) Lucenin-2 (B) Galangin (C) Spathulenol (D) Chalcone (E) Isocalamendiol (F) Isoacolamone. Standard antibiotic (G) Tecovirimat with binding energy −9.3 kcal/mol was utilized as control.

observed. Amino acid interactions of compounds with the highest affinities were quite similar to the controls (Mitoxantrone and Tecovirimat) (Supplementary Table S5). All the predicted interactions between the A42R and phytoconstituents having significant docking scores were mentioned in Supplementary Table S4 and Supplementary Fig. S4. Taken together, our results revealed that β-Sitosterol can bind effectively to the A42R protein of MPXV.

3.2. Analysis of drug-like properties

Supplementary Table S6 shows the assessment findings for the drug-like characteristics of chosen substances. Lipinski's rule of thumb states that substances that do not fulfill several standards have low oral bioavailability.[56,57] All nine of the compounds for 2V54, twelve for 4E9O, six for 4QWO, and five for 6BED satisfy all the Lipinski rules in our investigation, including those of MW ≤ 500, HBA ≤ 10, HBD ≤ 5, and Log P (octanol/water) < 5. The molecules Lucenin-2 for 4E9O and 6BED, (2S,3R,4R,5S,6S)-2-(hydroxymethyl)-6, and Lucenin-2 for 4QWO satisfy the Lipinski rule with just one permissible violation. In addition, the Veber and Egan guidelines were utilized to evaluate these substances. With each chemical achieving a bioavailability of about 55 %, most of them have outstanding bioavailability ratings.

3.3. ADMET properties analysis

Pharmacokinetic characteristics (PKs), which aid in understanding and forecasting biological effects such as a chemical's positive or negative influence on a certain system, are crucial to drug research. The drug compound's pharmacokinetic features assess if it was effectively absorbed from the digestive tract, precisely delivered to its intended location, sufficiently metabolized, and excreted from the body without creating any adverse effects. The absorption, distribution, metabolism, excretion, and toxicity (ADMET) properties of a molecule are critical in establishing its pharmacokinetics, which are critical phases in a drug's effectiveness. Supplementary Table S7 displays the findings of our investigation of ADMET characteristics. Exploring the ADME properties of the mentioned drugs, including water solubility, intestinal absorption in humans, blood–brain barrier permeability, and CYP1A2/CYP2C19/CYP2C9/CYP2D6/CYP3A4 inhibitors. Examining these attributes is necessary to ensure a medication's effectiveness by evaluating its biological activity and accurate delivery of the desired organ at a certain dosage. When the proportion of absorption by the human intestines is less than 30 %, it is considered low absorption. Every molecule had a human intestinal absorption (HIA) range of greater than 92 %, which is indicative of extremely high absorption rates. Lucenin-2 showed poor

Table 3
Phytoconstituents of *A. calamus* L. with higher docking scores and their amino acids interaction profile with viral capsid protein D13L (PDB ID: 6BED).

Receptor Name	Name of Compound	Docking Score (kcal/mol)	Types of interactions with amino acid residues				
			Van der Waals	Alkyl	Pi interactions	Conventional H-bond	Carbon-hydrogen bond
6BED	Lucenin-2	−9.2	ASN 96, 424 ILE 95, 428 GLU 111 GLY112, PRO 186, 426 ARG 234, ILE 236, LYS 260, TYR262,PHE 427,GLN 524		Pi-anion: ASP 189 Pi-alkyl:Pro 426	ASN 185, 268, PRO 261, 426, TYR 263,ASP 425	
	Galangin	−8.7	PRO 88, TYR 89,283 ASN 117, 435, 472 GLN 278, LYS 434		Pi-Cation: LYS 93, 429 Pi-Pi-T-shaped: TYR 116 Pi-alkyl: ILE 120	PHE 427, 433	ILE 428
	Spathulenol	−7.7	THR 30 ALA 65 THR 167 TYR 217, VAL 222	VAL 219	Pi-sigma: PHE 168 Pi-alkyl: TYR 32	SER 170	
	Chalcone	−7.6	THR 30, 167, 217 PHE 168 SER 170 LYS 172 VAL 222 GLN 223		Pi-sigma: VAL 219 PiPi-T shaped: TYR 32 Pi-alkyl:ALA 65,LYS 225		ILE 224
	Isocalamendiol	−7.5	PRO 88 ILE 120, 428 GLN 278 TYR 116, 283 PHE 427,ASN 435, 472,LYS 434	LYS 429	Pi-alkyl: TYR 89	ASP 425,PHE 433	
	Isoacolamone	−7.5	TYR 89,116, 283 LYS 93, 434, 472 ILE 120, 428 GLN 278 ASP 425, PHE 427, 433, ASN 435, 472	PRO 88			

absorption rate 3.38 % and [(1S,3R,5S,8S,9R,11R,14R,16S, 17R,18S,19S)-9,10,19-trihydroxy-5-methyl-12-methylidene-7-azahep tacyclo [9.6.2.01,8.05,17.07,16.09,14.014,18]nonadecan-3-yl] acetate showed moderate absorption rate 37.48 %.

Volume of distribution in humans (VDss) and blood–brain barrier (BBB) crossing capabilities were used to access the compound's dispersion. A drug's distribution is suggested to be lower if the logVDss value is < -0.15, and higher if it is >0.45. Most of the drugs had a volume of distribution that ranged from moderate to high. To shield the central nervous system (CNS), the blood–brain barrier blocks some substances (mostly dangerous ones) from penetrating the brain tissues. To maintain the homeostasis of CNS, the BBB controls the ingress of foreign substances. A few compounds can penetrate the blood–brain barrier (BBB), but the majority of compounds are considered prospective medication candidates based on the pkCSM recommendations. This is because they have a low probability of penetrating the BBB.

Cytochrome P450s are heme-containing enzymes that are involved in drug metabolism and detoxification of foreign substances (CYPs). Medications may function as cytochrome P450 enzyme inducers or inhibitors, which may result in medication interactions and unfavorable side effects or decreased therapeutic efficacy.[58] Analyzing a compound's influence on cytochrome P450 (CYP) is essential since CYP inhibitors can affect how drugs are metabolized. More than 90 % of drugs require the CYP types such as 1A2, 2C9, 2C19, 2D6, and 3A4 to be biotransformed during the first stage of metabolism. The effects of 2D6 and 3A4, two distinct variants, on drug metabolism are significant. One of the metabolites functioned as a CYP2D6 inhibitor throughout metabolism, whereas the other three were none of the substrates of CYP2D6. A small number of the substances that were investigated were determined to be strong CYP3A4 inhibitors, while very few were discovered to be CYP3A4 substrates. Furthermore, a small number of substances were shown to be potent CYP1A2, CYP2C19, and CYP2C9 inhibitors.

Since adverse side effects are frequently attributed to the failure of subsequent phases of drug development, drug toxicity is a major worry and a critical issue in the medical industry.[44] The potential harm that a chemical substance could do to an organism or any of its constituent parts, such as cells and organs, is measured by its toxicity. Therefore, it would be extremely beneficial to identify toxicity as soon as possible. Supplementary Table S7 presents the findings with respect to the possible toxicity of every compound under investigation. It is expected that none of the drugs will show AMES toxicity, hepatotoxicity, or hERGI and II (human Ether-a-go-go-related gene) suppression based on the results. It was confirmed that there was a high degree of safety and that these compounds are promising candidates for additional investigation based on the similarly encouraging evaluation of all the toxicity characteristics.

4. Discussion

The world witnessed recurring endemic and sporadic outbreaks of the Mpox disease in the last two decades. MPXV, a causative agent of Mpox clinically resembles smallpox. It is classified into two clades, Clade I and Clade II with each having its subclades.[59] Clade IIb is responsible

Table 4
Phytoconstituents of *A. calamus* L. with higher docking scores and their amino acids interaction profile with profilin-like protein A42R (PDB ID: 4QWO).

Receptor Name	Name of Compound	Docking Score (kcal/mol)	Types of interactions with amino acid residues				
			Van der Waals	Alkyl	Pi interactions	Conventional H-bond	Carbon-hydrogen bond
4QWO	beta-Sitosterol	−8.8	THR A:71, 79, SER A:73, GLU A:83, ARG A:114, ARG B:115, ASP B:123	ARG A:119, 122, ARG B:119, 122	Pi-alkyl:TYR A:118,TYR B:118		
	(2S,3R,4R,5S,6S)-2-(hydroxymethyl)-6-(((2S,3R,4R,5S,6R)-3,4,5-trihydroxy-6-(((4aR,8aS)-4-isopropyl-1,7-dimethyl-1,2,3,4,4a,5,8,8a-octahydronaphthalen-1-yl)oxy)tetrahydro-2H-pyran-2-yl)methoxy)tetrahydro-2H-pyran-3,4,5-triol	−8.7	ASN A:14, ASP A:116, 123 ARG A:119, THR A:120, TYR B:80, HIS B:100, ALA B:130, THR B:126	ILE A:11	Pi-alkyl:PHE A:17,HIS A:124	ASP A:10, ARG A:127, ASN B:78,ARG B:129	
	Lucenin-2	−8.5	SER A:73, THR A:79, TYR A:118, ARG A:119, ASN B:72, THR B:79, ALA B:81, GLU B:83, ARG B:114, 119, 122		Pi-Cation: ARG B:115, ARG A:115 Pi-alkyl:ARG B:115	ARG A:122, THR B:71, SER B:73,TYR B:118	
	[(1S,3R,5S,8S,9R,11R,14R,16S,17R,18S,19S)-9,10,19-trihydroxy-5-methyl-12-methylidene-7-azaheptacyclo [9.6.2.01,8.05,17.07,16.09,14.014,18]nonadecan-3-yl] acetate	−8	THR A:79, ARG A:122, THR B:79, ARG B:115, 122,TYR B:118			TYR A:118,ARG A:115, 119	ARG B:119
	(1S,4S)-1,4-dimethyl-7-propan-2-ylidene-1,2,3,4,5,8-hexahydroazulen-6-one	−7.7	GLU A:83, ARG A:114, 122,TYR B:118,ARG B:119, 122	ARG A:119	Pi-Sigma: TYR A:118 Pi-alkyl:TYR A:118		
	Arhimachalene	−7.7	GLU B:18, ASP B:19, ARG B:38, THR B:39, LYS B:65, THR B:86, TYR B:88, PRO B:90, 93, 110SER B:92,GLY B:108	ILE B:94	Pi-Pi T-shaped: PHE B:40		
	gamma-Diasarone	−7.7	ARG B:114	TYR A:118, ARG A:119, 122, ARG B:115, 119,TYR B:118,	Pi-Pi Stacked: TYR B:118	ARG B:122	ASP A:123, GLU B:83, TYR B:118, ASP B:123
	Thunbergol	−7.7	ARG A:119, 122,ARG B:115, 119, 122,TYR B:118		Pi-Sigma: TYR A:118 Pi-alkyl:TYR A:118		

for the higher rate of morbidity. Pathogenesis of pox viruses includes three major steps viz. attachment, membrane fusion, and core invasion.[60] After transmission of the MPXV, it attaches and fuses to the host cells through the virus uncoating and releasing its core structures into the cytoplasm of the infected host cells. Then after, the virus follows the pathway of early gene expression responsible for the beginning of viral mRNA synthesis and subsequent translation of viral proteins and enzymes used for replication such as DNA helicases and DNA primases, as well as structural proteins required for the assembly of new viral particles.[6] Following that, late gene expression occurs which promotes the assembly and maturation of virions by synthesis of other essential viral proteins such as membrane proteins, major capsid proteins, and proteins involved in viral morphogenesis. Subsequently, viral particles assemble and form intracellular mature viruses (IMV). In later stages,

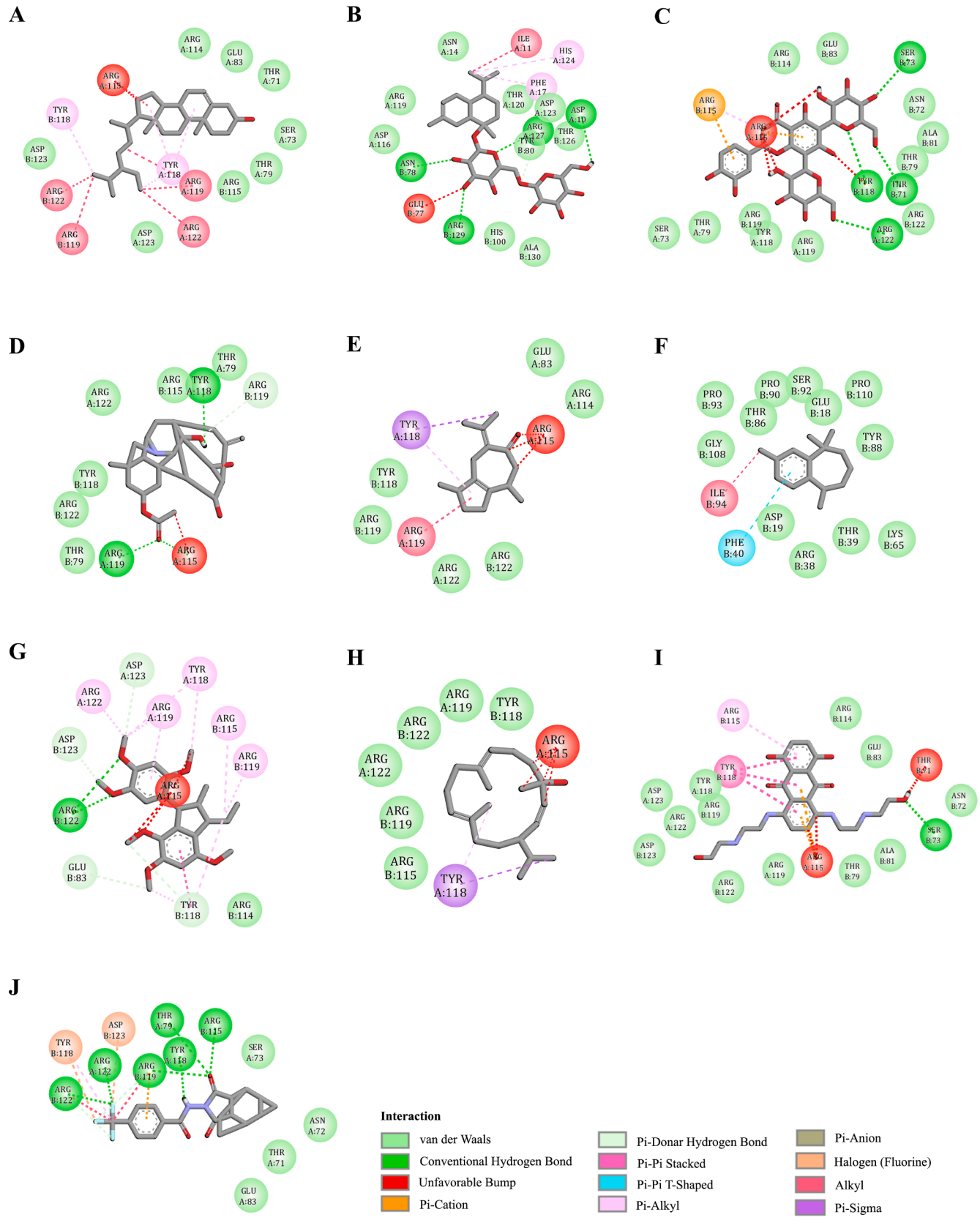

Fig. 4. Molecular 2D interaction of A42R (PDB ID: 4QWO) with phytoconstituents of *A. calamus* L. having binding energy ≤−7.7 kcal/mol (A) β-Sitosterol (B) (2S,3R,4R,5S,6S)-2-(hydroxymethyl)-6-(((2S,3R,4R,5S,6R)-3,4,5-trihydroxy-6-(((4aR,8aS)-4-isopropyl-1,7-dimethyl-1,2,3,4,4a,5,8,8a-octahydronaphthalen-1-yl) oxy)tetrahydro-2H-pyran-2-yl)methoxy)tetrahydro-2H-pyran-3,4,5-triol (C) Lucenin-2 (D) [(1S,3R,5S,8S,9R,11R,14R,16S,17R,18S,19S)-9,10,19-trihydroxy-5-methyl-12-methylidene-7-azaheptacyclo[9.6.2.01,8.05,17.07,16.09,14.014,18]nonadecan-3-yl] acetate (E) (1S,4S)-1,4-dimethyl-7-propan-2-ylidene-1,2,3,4,5,8-hexahydroazulen-6-one (F) Arhimachalene (G) gamma-Diasarone (H) Thunbergol. Standard antibiotics (I) Mitoxantrone with binding energy −7.4 kcal/mol and (J) Tecovirimat with binding energy −8.9 kcal/mol were utilized as control.

IMV is converted to the intracellular enveloped virus (IEV) which fuses with the host cell membrane and forms either the cell-associated enveloped virus (CEV) or the free extracellular enveloped virus (EEV). CEV and EEV infect neighboring cells and release in the tissue fluid respectively and resulting in the spread of the infection.[7] The molecular mechanism of viral replication is tightly regulated and synchronized by viral proteins, which interact with the host cell to control cellular processes and support viral replication. D8L, a membrane protein, binds to the host cell surface receptor chondroitin sulfate and facilitates its entry via membrane fusion or endocytosis.[61] A48R, a thymidylate kinase participates in nucleotide metabolism.[52] Currently, no approved inhibitors are available against A48R, which makes it a prominent therapeutic target.[62–63] The D13L, is responsible for the morphogenesis of immature virions to mature viruses.[64] Rifampin targets D13L and arrests the virion morphogenesis reversibly and hence is not approved as a standard drug for MPXV.[65] Furthermore, A42R, a profilin-like protein interacts with host actin and alpha-tropomycin and augments cytoskeletal dynamics leading to viral spread to adjoining cells.[66] Earlier reports suggest that these proteins have been utilized as a potential drug target to combat MPXV.[67–70] Currently, some vaccinia vaccines and FDA-approved antiviral compounds are used to treat MPXV infection but they exhibit adverse effects and lack adequate data for their efficacy in humans.[71].

A Plethora of medicinal plants and their secondary metabolites have a wide range of biological activities.[72,73] Many of them are being studied in modern research to discover an active drug candidate. AC is a well-known medicinal plant utilized to treat a wide range of health issues, including neurological, gastrointestinal, respiratory, metabolic, kidney, and liver disorders since Vedic time.[74] The rhizomes, roots, and essential oils of AC have been reported to possess various important phytoconstituents such as α-Asarone, β-Asarone, Cis and Trans isoeugenol, *cis*-Isoelemicine, β-Cadinene, Terpinen-4-ol, Terpineol, Camphor, Camphene, P-Cymene, α-Selinene, Acoragermacrone, β-Gurjunene, Anddienol, Shyobunones, 2-deca-4,7-Linalool and Preisocalamendiol, Galangin, 2,5-dimethoxy benzoquinone, 2,4,5-trimethoxybenzaldehyde, Calamendiol, Spathulenol and Sitosterol which possess plethora of bioactivities.[29,47,75,76] However, its antiviral activities have been under-explored. Here, we have uncovered crucial insight into the binding affinity and interaction between the selected target proteins D8L, A48R, D13L, and A42R and 255 phytoconstituents of AC through an *in silico* molecular docking study. FDA-approved drugs Cidofovir, Brincidofovir, and Tecovirimat exhibit antiviral activity against Orthopoxviruses and hence we utilized them as controls in the present study.[71] Further, we have evaluated their ADMET properties to understand the safety and efficacy of phytoconstituents. Our findings suggest that phytoconstituents such as Galangin, Chalcone, and Benzyl benzoate could be good as antiviral compounds targeting MPXV.

Our findings revealed that among the all-screened phytoconstituents β-Sitosterol, Lucenin-2, Galangin, and Mukulol displayed the highest binding affinity about protein D8L. The binding site pocket of D8L consists of amino acid residues such as GLY 40, LYS 41, LEU 42, ARG 44, SER 64, THR 65, HIS 67, TYR 69, VAL 94, TYR 104, LYS 108, ILE 116, THR 173, ILE 174, ASN 175, SER 177, TRP 182, SER 204, SER 205, ASN 207, HIS 208, HIS 213, TYR 214, ILE 215, THR 216, GLU 217, ASN 218, TYR 219, ARG 220, and ASN 221. The residue ASN 175 plays an important role in interaction with the host cell.[77,78] β-Sitosterol, Galangin, Mukulol, (+)-delta-Cadinene, Chalcone, (−)-alpha-Cadinol, (1S,4S)-1,4-dimethyl-7-propan-2-ylidene-1,2,3,4,5,8-hexahydroazulen-6-one, β-Cubebene, and Heterotropan interact with ASN 175 through van der Waals interactions. Additionally, Lucenin- 2, [(1S,3R,5S,8S, 9R,11R,14R,16S,17R,18S,19S) 9,10,19-trihydroxy-5-methyl-12-methylidene-7 azaheptacyclo [9.6.2.01,8.05,17.07,16.09,14.014,18] nona decan-3-yl] acetate form favorable conventional hydrogen bonds with ASN 175 and *cis*-Calamenen-10-ol form hydrophobic bonds with ASN 175. Other amino acids of binding sites such as THR 173, ARG 44, TYR 69, ILE 174, ASN 175, HIS 67, and LEU 42 are involved in the complex of almost all phytoconstituents with D8L. These interactions show the stability of bound phytoconstituents in the binding groove of protein.

Phytoconstituents derived from AC also showed significant potency against the viral protein A48R. Compounds such as Zingiberene, β-Bisabolene, Galangin, (+)-delta-Selinene, Benzyl benzoate, Indane, 1-phenyl, alpha-Selin(−)-β-Curcumene, and Chalcone exhibit exceptionally higher affinity with lowest binding scores. These compounds interact with amino acids of the active site through either hydrogen bonds or hydrophobic bonds. As per the literature, active site residues of A48R are ASN 65, LEU 111, LYS 105, ALA 107, and TYR 144.[52,62] Zingiberene, β-Bisabolene, Benzyl benzoate, and (−)-β-Curcumene interact with ASN 65 through van der Waals interaction, along with hydrophobic interactions with the LYS 105 and TYR 144. Other phytoconstituents only bind through van der Waals interactions with TYR 144. PHE 68, ARG 93, and GLU 142 are important amino acids interacting by hydrogen bonds, pi-pi stacking, pi-cation interaction, and salt bridges.[79] Zingiberene, β-Bisabolene, Galangin, (+)-delta-Selinene, alpha-Selinene, (−)-β-Curcumene, and Chalcone formed either hydrogen or hydrophobic bonds with all three amino acids viz. PHE 68, ARG 93, and GLU 142. The above results showed that phytoconstituents such as Zingiberene, β-Bisabolene, Galangin, (+)-delta-Selinene, alpha-Selinene, (−)-β-Curcumene, and Chalcone may act as promising inhibitors for A48R. In our investigation, phytoconstituents potentially bound to the capsid protein D13L of MPXV with significantly lower binding energies.

Furthermore, protein A42R displayed stable interactions with the ligands. Our findings revealed that β-Sitosterol, (2S,3R,4R,5S,6S)-2-(hydroxymethyl)-6-(((2S,3R,4R,5S,6R)-3,4,5-trihydroxy-6-(((4aR,8aS)-4-isopropyl-1,7-dimethyl-1,2,3,4,4a,5,8,8a-octahydronaphthalen-1-yl) oxy)tetrahydro-2H-pyran-2-yl)methoxy)tetrahydro-2H-pyran-3,4,5-triol, Lucenin-2, [(1S,3R,5S,8S,9R,11R,14R,16S,17R,18S,19S)-9,10,19-trihydroxy-5-methyl-12-methylidene-7-azaheptacyclo[9.6.2.01,8.05, 17.07,16.09,14.014,18]nonadecan-3-yl] acetate, (1S,4S)-1,4-dimethyl-7-propan-2-ylidene-1,2,3,4,5,8-hexahydroazulen-6-one, Arhimachalene, gamma-Diasarone and Thunbergol bound to A42R with low binding affinity and these complexes were stabilized by various hydrogen and hydrophobic interactions. Previous reports suggested that GLU 83, TYR 118, ARG 114, ARG 115, ARG 119, ARG 122, and ASP 123 are the binding site amino acids of A42R.[80] AC phytoconstituent β-Sitosterol interacts with all these amino acids through van der Waals or Pi Alkyl/Alkyl bonds. Lucenin-2 forms conventional hydrogen bonds with amino acids ARG 122 and TYR 119, hydrophobic bonds with amino acid ARG 115, and van der Waals interactions with amino acids GLU 83, TYR 118, ARG 114, ARG 119, and ARG 122.

Among all screened phytoconstituents, several demonstrate strong interactions with multiple targets of MPXV, highlighting its potential as a broad-spectrum therapeutic agent against MPXV. For example, Galangin interacts with all selected targets with lower binding energy (−6.9 kcal/mol, −8.5 kcal/mol, −8.7 kcal/mol, −7.4 kcal/mol) and higher affinity. Likewise, Chalcone and Benzyl benzoate interact efficiently with three targets D13L, D8L, and A48R with the docking score range between −6.5 kcal/mol to −8.2 kcal/mol. Many phytoconstituents displayed strong affinities with lower binding energy against dual protein targets (Supplementary Table S8).

Inhibition parameters alone cannot qualify a compound as a potential drug candidate. Physicochemical, drug-likeness, and ADMET properties are also needed for deciding the bio-suitability of the potent drug candidates. In our study, all top compounds followed Lipinski's rule of 5 and showed good pharmacokinetic properties.

5. Conclusion

Mpox is an infectious viral disease caused by MPXV. Nowadays, due to its rapid prevalence, there is an urgent need for the identification or development of novel antivirals that inhibit important proteins involved in any stage of the MPXV life cycle. In the present study, we evaluated

the potency of 255 phytoconstituents from AC against protein targets (A42R, D8L, D13L and A48R) of MPXV through a molecular docking study. The docking study revealed that compound β-Sitosterol has the highest affinity to the targets A42R and D8L. Furthermore, Lucenin-2 and Zingiberene bind with the target D13L and A48R respectively through the lowest binding energy and maximum affinity. Galangin was identified as a potential phytoconstituent as it exhibited strong binding affinity toward all four target proteins of MPXV. Based on the docking study, we can hypothesize that these phytoconstituents can act as inhibitors of MPXV target proteins. ADMET studies showed that all phytoconstituents have acceptable drug-likeness, pharmacological properties, and suitability as drug candidates. Moreover, due to their natural existence, bioactive phytoconstituents offer a promising substitute for existing antivirals that have adverse side effects. We recommend *in vitro* and *in vivo* validation of our findings as an opportunity to develop the Mpox therapeutic regimen.

CRediT authorship contribution statement

Shivani Lakhani: Writing – original draft, Software, Methodology, Investigation, Formal analysis, Data curation. **Janki V. Rojmala:** Writing – original draft, Software, Methodology, Investigation, Formal analysis, Data curation. **Nisarginee M. Chotai:** Writing – original draft, Software, Formal analysis. **Bhargav N. Waghela:** Writing – review & editing, Writing – original draft, Supervision, Conceptualization. **Parth Thakor:** Writing – review & editing, Writing – original draft, Supervision, Software, Resources, Project administration, Methodology, Investigation, Formal analysis, Data curation, Conceptualization.

Declaration of competing interest

The authors declare that they have no known competing financial interests or personal relationships that could have appeared to influence the work reported in this paper.

Acknowledgments

We are thankful to Bapubhai Desaibhai Patel Institute of Paramedical Sciences (BDIPS), Charotar University of Science and Technology, Changa, and Atmiya University, Rajkot for providing infrastructure facilities.

Appendix A. Supplementary material

Supplementary data to this article can be found online at https://doi.org/10.1016/j.jgeb.2025.100487.

References

1. McFadden G. Poxvirus tropism. *Nat Rev Microbiol*. 2005;3(3):201–213.
2. Brown K, Leggat PA. Human monkeypox: current state of knowledge and implications for the future. *Tropical Med Infect Dis*. 2016;1(1):8.
3. Mitjà O, Ogoina D, Titanji BK, et al. Monkeypox. *Lancet*. 2023;401(10370):60–74.
4. Rabaan AA, Alwashmi AS, Mashraqi MM, et al. Cheminformatics and machine learning approaches for repurposing anti-viral compounds against monkeypox virus thymidylate kinase. *Mol Divers*. 2023;1–14.
5. Ola P. The origin of the mysterious multi-country monkeypox outbreak in non-endemic countries. 2022.
6. Alakunle E, Moens U, Nchinda G, Okeke MI. Monkeypox virus in Nigeria: infection biology, epidemiology, and evolution. *Viruses*. 2020;12(11):1257.
7. Veintimilla C, Catalán P, Alonso R, et al. The relevance of multiple clinical specimens in the diagnosis of monkeypox virus, Spain, June 2022. *Eurosurveillance*. 2022;27(33), 2200598.
8. Ulaeto D, Agafonov A, Burchfield J, et al. New nomenclature for mpox (monkeypox) and monkeypox virus clades. *Lancet Infect Dis*. 2023;23(3):273–275.
9. Gong Q, Wang C, Chuai X, Chiu S. Monkeypox virus: a re-emergent threat to humans. *Virol Sin*. 2022;37(4):477–482.
10. Falcinelli SD, Chertow DS, Kindrachuk J. Integration of global analyses of host molecular responses with clinical data to evaluate pathogenesis and advance therapies for emerging and re-emerging viral infections. *ACS Infect Dis*. 2016;2(11):787–799.
11. Uwishema O, Adekunbi O, Peñamante CA, et al. the burden of monkeypox virus amidst the Covid-19 pandemic in Africa: a double battle for Africa. *Annals Med Surg*. 2022;80.
12. Matho MH, Maybeno M, Benhnia M-R-E-I, et al. Structural and biochemical characterization of the vaccinia virus envelope protein D8 and its recognition by the antibody LA5. *J Virol*. 2012;86(15):8050–8058.
13. Chaurasiya S, Chen NG, Lu J, et al. A chimeric poxvirus with J2R (thymidine kinase) deletion shows safety and anti-tumor activity in lung cancer models. *Cancer Gene Ther*. 2020;27(3):125–135.
14. Ezat AA, Abduljalil JM, Elghareib AM, Samir A, Elfiky AA. The discovery of novel antivirals for the treatment of mpox: is drug repurposing the answer? *Expert Opin Drug Discov*. 2023;18(5):551–561.
15. Moss B. Poxvirus DNA replication. *Cold Spring Harb Perspect Biol*. 2013;5(9), a010199.
16. Ashley CN, Broni E, Wood CM, et al. Identifying potential monkeypox virus inhibitors: an in silico study targeting the A42R protein. *Front Cell Infect Microbiol*. 2024;14, 1351737.
17. Smith GL, Benfield CT, Maluquer de Motes C, et al. Vaccinia virus immune evasion: mechanisms, virulence and immunogenicity. *J Gen Virol*. 2013;94(11):2367–2392.
18. Suraweera CD, Hinds MG, Kvansakul M. Poxviral strategies to overcome host cell apoptosis. *Pathogens*. 2020;10(1):6.
19. Shchelkunov SN. Orthopoxvirus genes that mediate disease virulence and host tropism. *Adv Virol*. 2012;2012(1), 524743.
20. Sergey S, Shchelkunova G. Genes that control vaccinia virus immunogenicity. *Acta Nat (англоязычная Версия)*. 2020;121(44):33–41.
21. Nichols DB, De Martini W, Cottrell J. Poxviruses utilize multiple strategies to inhibit apoptosis. *Viruses*. 2017;9(8):215.
22. Yu H, Bruneau RC, Brennan G, Rothenburg S. Battle royale: innate recognition of poxviruses and viral immune evasion. *Biomedicines*. 2021;9(7):765.
23. Organization WH. Strategic advisory group of experts on immunization (SAGE). URL: https://www who int/immunization/policy/sage/en/ (date of access-0111 2022). 2020.
24. Grabenstein JD, Hacker A. Vaccines against Mpox: MVA-BN and LC16m8. *Expert Rev Vaccines*. 2024. just-accepted.
25. O'Laughlin K. Clinical use of tecovirimat (Tpoxx) for treatment of monkeypox under an investigational new drug protocol—United States, May–August 2022. *MMWR Morb Mortal Wkly Rep*. 2022;71(37):1190–1195. https://doi.org/10.15585/mmwr.mm7137e1.
26. Siegrist EA, Sassine J. Antivirals with activity against mpox: a clinically oriented review. *Clin Infect Dis*. 2023;76(1):155–164.
27. Khwairakpam AD, Damayenti YD, Deka A, et al. Acorus calamus: a bio-reserve of medicinal values. *J Basic Clin Physiol Pharmacol*. 2018;29(2):107–122.
28. Sharma V, Sharma R, Gautam DS, Kuca K, Nepovimova E, Martins N. Role of Vacha (Acorus calamus Linn.) in neurological and metabolic disorders: evidence from ethnopharmacology, phytochemistry, pharmacology and clinical study. *J Clin Med*. 2020;9(4):1176.
29. Ganjewala D, Srivastava AK. An update on chemical composition and bioactivities of Acorus species. *Asian J Plant Sci*. 2011;10(3):182.
30. Huang Y, Li Z, Ma Y, et al. Screening for active compounds of acorus calamus against SARS-CoV-2 viral protease and mechanism prediction. *Pharmaceuticals*. 2024;17(3):325.
31. Kwofie SK, Broni E, Teye J, et al. Pharmacoinformatics-based identification of potential bioactive compounds against Ebola virus protein VP24. *Comput Biol Med*. 2019;113, 103414.
32. Yao X, Ling Y, Guo S, et al. Tatanan A from the Acorus calamus L. root inhibited dengue virus proliferation and infections. *Phytomedicine*. 2018;42:258–267.
33. Pathania S, Randhawa V, Kumar M. Identifying potential entry inhibitors for emerging Nipah virus by molecular docking and chemical-protein interaction network. *J Biomol Struct Dyn*. 2020;38(17):5108–5125.
34. Zardecki C, Dutta S, Goodsell DS, Lowe R, Voigt M, Burley SK. PDB-101: Educational resources supporting molecular explorations through biology and medicine. *Protein Sci*. 2022;31(1):129–140.
35. Biovia DS. Discovery studio. *Dassault Systèmes BIOVIA*. 2016.
36. Dallakyan S, Olson AJ. Small-molecule library screening by docking with PyRx. *Chem Biol: Methods Protocols*. 2015:243–250.
37. Vivek-Ananth R, Mohanraj K, Sahoo AK, Samal A. IMPPAT 2.0: An enhanced and expanded phytochemical atlas of Indian medicinal plants. *ACS Omega*. 2023;8(9):8827–8845.
38. Wermuth CG, Villoutreix B, Grisoni S, Olivier A, Rocher J-P. Strategies in the search for new lead compounds or original working hypotheses. In: *The practice of medicinal chemistry*. Elsevier; 2015:73–99.
39. Morris GM, Lim-Wilby M. Molecular docking. Molecular modeling of proteins. 2008:365-382.
40. Lam T-P, Tran V-H, Mai TT, et al. Identification of diosmin and flavin adenine dinucleotide as repurposing treatments for monkeypox virus: a computational study. *Int J Mol Sci*. 2022;23(19):11570.
41. Preet G, Oluwabusola ET, Milne BF, Ebel R, Jaspars M. Computational repurposing of mitoxantrone-related structures against monkeypox virus: a molecular docking and 3D pharmacophore study. *Int J Mol Sci*. 2022;23(22):14287.
42. Sahoo AK, Augusthian PD, Muralitharan I, et al. In silico identification of potential inhibitors of vital monkeypox virus proteins from FDA approved drugs. *Mol Divers*. 2023;27(5):2169–2184.
43. Daina A, Michielin O, Zoete V. SwissADME: a free web tool to evaluate pharmacokinetics, drug-likeness and medicinal chemistry friendliness of small molecules. *Sci Rep*. 2017;7(1):42717.

44. Lipinski CA, Lombardo F, Dominy BW, Feeney PJ. Experimental and computational approaches to estimate solubility and permeability in drug discovery and development settings. *Adv Drug Deliv Rev*. 2012;64:4–17.
45. Veber DF, Johnson SR, Cheng H-Y, Smith BR, Ward KW, Kopple KD. Molecular properties that influence the oral bioavailability of drug candidates. *J Med Chem*. 2002;45(12):2615–2623.
46. Egan WJ, Merz KM, Baldwin JJ. Prediction of drug absorption using multivariate statistics. *J Med Chem*. 2000;43(21):3867–3877.
47. Thakkar SS, Shelat F, Thakor P. Magical bullets from an indigenous Indian medicinal plant Tinospora cordifolia: an in silico approach for the antidote of SARS-CoV-2. *Egypt J Pet*. 2021;30(1):53–66.
48. Namera DL, Thakkar SS, Thakor P, Bhoya U, Shah A. Arylidene analogues as selective COX-2 inhibitors: synthesis, characterization, in silico and in vitro studies. *J Biomol Struct Dyn*. 2021;39(18):7150–7159.
49. Thakor P, Subramanian RB, Thakkar SS, Ray A, Thakkar VR. Phytol induces ROS mediated apoptosis by induction of caspase 9 and 3 through activation of TRAIL, FAS and TNF receptors and inhibits tumor progression factor Glucose 6 phosphate dehydrogenase in lung carcinoma cell line (A549). *Biomed Pharmacother*. 2017;92:491–500.
50. Socha BN, Pandya SB, Patel UH, et al. 1-D MOF [Ag2 (C10H10N3O3S) 2 (C4H8N) 2] n: Photocatalytic treatment, crystallographic evaluation, ADMET parameters, CT-DNA and anticancer activity. *J Biomol Struct Dyn*. 2024;42(13):6925–6940.
51. Das R, Bhattarai A, Karn R, Tamang B. Computational investigations of potential inhibitors of monkeypox virus envelope protein E8 through molecular docking and molecular dynamics simulations. *Sci Rep*. 2024;14(1):19585.
52. Caillat C, Topalis D, Agrofoglio LA, et al. Crystal structure of poxvirus thymidylate kinase: an unexpected dimerization has implications for antiviral therapy. *Proc Natl Acad Sci*. 2008;105(44):16900–16905.
53. Hyun J, Matsunami H, Kim TG, Wolf M. Assembly mechanism of the pleomorphic immature poxvirus scaffold. *Nat Commun*. 2022;13(1):1704.
54. Elmezayen AD, Al-Obaidi A, Şahin AT, Yelekçi K. Drug repurposing for coronavirus (COVID-19): in silico screening of known drugs against coronavirus 3CL hydrolase and protease enzymes. *J Biomol Struct Dyn*. 2021;39(8):2980–2992.
55. Topalis D, Collinet B, Gasse C, et al. Substrate specificity of vaccinia virus thymidylate kinase. *FEBS J*. 2005;272(24):6254–6265.
56. Kalita J, Chetia D, Rudrapal M. Molecular docking, drug-likeness studies and ADMET prediction of quinoline imines for antimalarial activity. *J Med Chem Drug Des*. 2019;2(1):1–7.
57. Thakkar SS, Thakor P, Ray A, Doshi H, Thakkar VR. Benzothiazole analogues: synthesis, characterization, MO calculations with PM6 and DFT, in silico studies and in vitro antimalarial as DHFR inhibitors and antimicrobial activities. *Bioorg Med Chem*. 2017;25(20):5396–5406.
58. Bultum LE, Tolossa GB, Kim G, Kwon O, Lee D. In silico activity and ADMET profiling of phytochemicals from Ethiopian indigenous aloes using pharmacophore models. *Sci Rep*. 2022;12(1):22221.
59. Kumar R, Nagar S, Haider S, Sood U, Ponnusamy K, Dhingra GG, et al. Monkey pox virus (MPXV): phylogenomics, host-pathogen interactome, and mutational cascade. *bioRxiv*. 2022.
60. Laliberte JP, Weisberg AS, Moss B. The membrane fusion step of vaccinia virus entry is cooperatively mediated by multiple viral proteins and host cell components. *PLoS Pathog*. 2011;7(12), e1002446.
61. Weaver JR, Isaacs SN. Monkeypox virus and insights into its immunomodulatory proteins. *Immunol Rev*. 2008;225(1):96–113.
62. Lam HYI, Guan JS, Mu Y. In silico repurposed drugs against monkeypox virus. *Molecules*. 2022;27(16):5277.
63. Prichard MN, Kern ER. Orthopoxvirus targets for the development of new antiviral agents. *Antiviral Res*. 2012;94(2):111–125.
64. Hyun J-K, Accurso C, Hijnen M, et al. Membrane remodeling by the double-barrel scaffolding protein of poxvirus. *PLoS Pathog*. 2011;7(9), e1002239.
65. Yuen In HL, Sheng GJ, Yuguang M. In silico repurposed drugs against monkeypox virus. *bioRxiv*. 2022.
66. Butler-Cole C, Wagner MJ, Da Silva M, Brown GD, Burke RD, Upton C. An ectromelia virus profilin homolog interacts with cellular tropomyosin and viral A-type inclusion protein. *Virol J*. 2007;4:1–15.
67. Gulati P, Chadha J, Harjai K, Singh S. Targeting envelope proteins of poxviruses to repurpose phytochemicals against monkeypox: an in silico investigation. *Front Microbiol*. 2023;13, 1073419.
68. Karataş H, Kiliç HK, Tüzün B, Kökbudak Z. Schiff base derivatives against monkeypox virus: synthesis, in silico, MM-GBSA and SAR properties. *J Mol Struct*. 2024;1298, 137073.
69. Mohapatra RK, Mahal A, Ansari A, et al. Comparison of the binding energies of approved mpox drugs and phytochemicals through molecular docking, molecular dynamics simulation, and ADMET studies: an in silico approach. *J Biosafe Biosecurity*. 2023;5(3):118–132.
70. Pourhajibagher M, Bahador A. Natural photosensitizers potentiate the targeted antimicrobial photodynamic therapy as the Monkeypox virus entry inhibitors: an in silico approach. *Photodiagn Photodyn Ther*. 2023;43, 103656.
71. Grosenbach DW, Honeychurch K, Rose EA, et al. Oral tecovirimat for the treatment of smallpox. *N Engl J Med*. 2018;379(1):44–53.
72. Beeby E, Magalhães M, Poças J, et al. Secondary metabolites (essential oils) from sand-dune plants induce cytotoxic effects in cancer cells. *J Ethnopharmacol*. 2020;258, 112803.
73. Elshafie HS, Camele I, Mohamed AA. A comprehensive review on the biological, agricultural and pharmaceutical properties of secondary metabolites based-plant origin. *Int J Mol Sci*. 2023;24(4):3266.
74. Rajput SB, Tonge MB, Karuppayil SM. An overview on traditional uses and pharmacological profile of Acorus calamus Linn.(Sweet flag) and other Acorus species. *Phytomedicine*. 2014;21(3):268–276.
75. Thakkar AB, Sargara P, Subramanian RB, Thakkar VR, Thakor P. Induction of apoptosis in lung carcinoma cells (A549) by hydromethanolic extract of Acorus calamus L. *Process Biochem*. 2022;123:1–10.
76. Chandra D, Prasad K. Phytochemicals of Acorus calamus (Sweet flag). *J Med Plants Stud*. 2017;5(5):277–281.
77. Altayb HN. Fludarabine, a potential DNA-dependent RNA polymerase inhibitor, as a prospective drug against monkeypox virus: a computational approach. *Pharmaceuticals*. 2022;15(9):1129.
78. Schoeniger JS, Hadi MZ, Light YK, Roe DC, Ayson M, Segelke B, et al. Structural Basis of Poxvirus Interaction with Cell-Surface Receptors and Synthetic Ligands. Sandia National Lab.(SNL-CA), Livermore, CA (United States); 2008.
79. Lokhande KB, Shrivastava A, Singh A. Discovery of potent inhibitors against monkeypox's major structural proteins using high throughput virtual screening, large scale molecular dynamics and DFT calculations. 2022.
80. Bajrai LH, Alharbi AS, El-Day MM, Bafaraj AG, Dwivedi VD, Azhar EI. Identification of antiviral compounds against monkeypox virus profilin-like protein A42R from plantago lanceolata. *Molecules*. 2022;27(22):7718.